Time-frequency analysis of spontaneous fluctuation of the pupil size of the human eye

Wioletta NOWAK[1], Andrzej HACHOŁ[1], Henryk KASPRZAK[2]

[1]Faculty of Basic Problems of Technology, Institute of Biomedical Engineering and Instrumentation, Wrocław University of Technology, Wybrzeże Wyspiańskiego 27, 50-370 Wrocław, Poland

[2]Faculty of Basic Problems of Technology, Institute of Physics, Wrocław University of Technology, Wybrzeże Wyspiańskiego 27, 50-370 Wrocław, Poland

Corresponding authors: W. Nowak – Wioletta.Nowak@pwr.wroc.pl; A. Hachoł – Andrzej.Hachol@pwr.wroc.pl; H. Kasprzak – Henryk.Kasprzak@pwr.wroc.pl

The aim of this work has been to develop a new method of variability description for the spontaneous pupillary fluctuation (SPF) signal, based on the time-frequency analysis. In the work we have studied the variability of the SPF signal spectrum. Based on the KPSS (Kwiatkowski, Philips, Schmidt, Shin) test, it has been shown that the SPF signal is non-stationary. A method of SPF signal variability analysis has been proposed using the STFT in the time--frequency domain, and then quantitative variability measures have been introduced to the obtained spectrograms. The application of fast pupillometry for recording the SPF allowed to expand the analyzed frequency band to 20 Hz. The proposed method of analysis and introduced measures of SPF variability enable the detection and quantitative description of short-lasting time-frequency and time-amplitude variations that remain obscured by the overall spectral analysis. SPF signal analysis methods and exemplary results obtained with the methods are presented in the paper.

Keywords: spontaneous pupillary fluctuation, spectral analysis, time-frequency representation, signal nature.

1. Introduction

The phenomenon of spontaneous pupillary fluctuation (SPF) appears in the conditions of permanent lighting and eye fixation, and it represents a dynamic equilibrium of pupil size for which the sympathetic and parasympathetic activity modulated by central nervous system is responsible. The detection of sleepiness-related fluctuations of pupil size in darkness by Lowenstein *et al*. [1] initiated the interest in applying this phenomenon in clinical studies. Unfortunately, progress in this area was limited because of methodological and technical problems. Today, infrared video pupillography enables not only stable long-time recordings of pupil size, but also numerical

quantification of SPF signal. The analysis of the SPF signal is used for monitoring the level of alertness in the clinical conditions [1–4], for diagnosing sleep disorders, and for assessing the efficacy of therapeutic interventions [5–11]. As a qualitative test, the pupillographic sleepiness test (PST) is used in the studies [7, 8, 12, 13]. During the PST, the SPF signal is being recorded for 11 minutes and next, after eliminating the artefacts, the SPF signal is subjected to the properly designed spectral analysis in the range of up to 0.8Hz (slow changes in pupil size), reflecting the level of vigilance. The analysis provides information on the frequency profile of the signal, on variations in the average pupil diameter, and on the tendency for pupil unrest. The aim of the analysis presented in [14–17] was to identify the SPF signal spectrum components. In the analysed spectrum range (up to 0.6 Hz) two important components were identified: the first one corresponding to baroreflex control, and the second one corresponding to respiratory component.

In our opinion, Fourier transform (FT), which is commonly used in the spectral analysis of SPF, has limitations in that signal testing. The SPF signal is non-stationary, *i.e.* its spectrum is varying in time, while the FT requires a stationary signal. The FT determines the averaged spectrum, not actually showing possible variations of that spectrum in time. Assuming that the studied SPF is stationary seems, at least in some cases, to be too big simplification. The combined time-frequency analysis is an important tool for non-stationary signals (*i.e.*, signals with time-varying spectra) where spectral characteristics of signals do not provide unique representations. Time-varying spectra of non-stationary time-series commonly used are spectrograms from the short-time Fourier transform (STFT). The extraction of time-frequency information with the STFT method has previously been applied in the analysis of other biological signals, including heart rate variability signal [18], corneal displacement [19] and gastric slow waves [20].

For studying spectral characteristics of the SPF signal, a time-frequency analysis using the STFT has been applied. For comparison, a standard FT analysis has also been performed. The SPF signal and its derivative, DSPF, representing speed of pupillary fluctuation have been subjected to the analysis.

2. Data analysis

The analysis has been performed offline, using the software written in Matlab 7.1, on 1080 data points, which were produced from the 12 second long record of the SPF registered with frequency 90 Hz. Length of the analysed signal is marked as *k*. Frequency resolution of the spectrum was determined as (1/1080)×90, which gives bin width of 0.083 Hz in frequency spectrum. The process of the analysis consisted of three stages: pre-processing, stationary analysis and spectral analysis. SPF and DSPF signals were studied. Since the DSPF signal contains some peaks related to recording errors, additionally it has been proposed to remove those speed values, which exceed certain, individually set values for each case. The values differed for various subjects and oscillated within the 0.1 to 0.3 mm/s range. Stationarity of SPF and DSPF signals

has been checked. For stationarity evaluation, the KPSS (Kwiatkowski, Philips, Schmidt, Shin) test [21] was used.

The Yule–Walker's method was used for determining the power spectral density (PSD). Four parameters have been used for comprising obtained PSD characteristics: PSD_1 (PSD value within the range of up to 1 Hz), PSD_2 (PSD value within the range of 1 Hz–2 Hz), PSD_3 (PSD value within the range of $2-10$ Hz) and PSD_4 (PSD value within the whole range). A short-window Fourier transform with Hamming window of the length equal to $k/4$ was used for time-frequency analysis.

Two methods were used for a quantitative description of obtained spectrograms. The first method of the quantitative spectrogram description consists in determining and analysing the variability of two parameters – power instability factor (PIF), and frequency instability factor (FIF). The principle for determining those parameters has been presented in Fig. 1**a**.
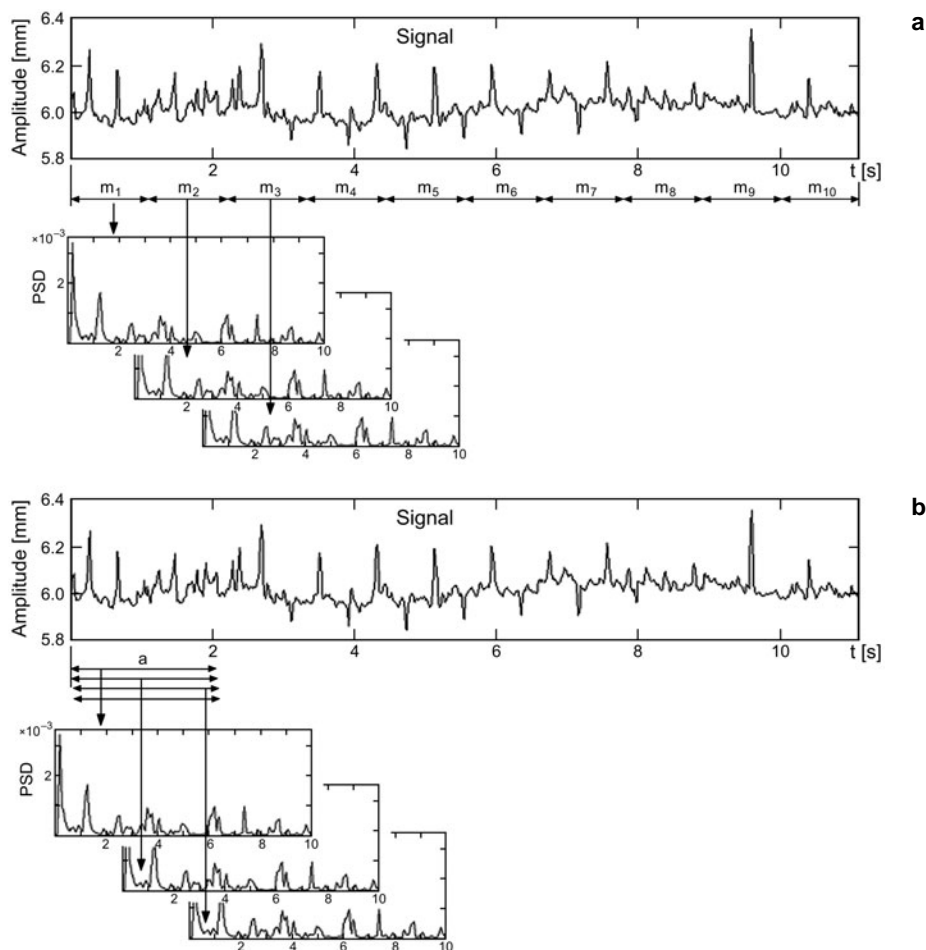

Fig. 1. Way of determining the instability factor values (**a**) and the PSD transient response (**b**).

The analyzed signal is being divided into $m = 10$ intervals of $n = 108$ samples each. For each interval i (i from 1 to $i = m$) a PSD characteristic is being determined. Frequency resolution of the spectrum was determined as $(1/108) \times 90$, which gives a bin width of 0.83 Hz in frequency spectrum. Each m characteristic is searched for a peak of maximum amplitude, finding its value ($P_{i\max}$) and the frequency for which the peak appears ($f_{i\max}$). As a result, $m = 10$ peak values of power and frequency are found. Next, percentage share of the $P_{i\max}$ peak in PSD value within the whole range (PSD$_4$) is calculated according to the following equation:

$$P_{i\max\%} = \frac{P_{i\max}}{\mathrm{PSD}_4} \times 100\% \tag{1}$$

The obtained 10 values of power percentage ($P_{i\max\%}$) and 10 values of frequency ($f_{i\max}$) are treated as a series and their average value and standard deviation are determined from the following equations:

$$\overline{P_{\max\%}} = \frac{\sum_{i=1}^{m} P_{i\max\%}}{m}; \quad \mathrm{SD}_{\overline{P_{\max\%}}} = \sqrt{\frac{\sum_{i=1}^{m} (P_{i\max\%} - \overline{P_{\max\%}})^2}{n(n-1)}} \tag{2}$$

$$\overline{f_{\max}} = \frac{\sum_{i=1}^{m} f_{i\max}}{m}; \quad \mathrm{SD}_{\overline{f_{\max}}} = \sqrt{\frac{\sum_{i=1}^{m} (f_{i\max} - \overline{f_{\max}})^2}{n(n-1)}} \tag{3}$$

Instability factors are defined as a ratio of standard deviation (accordingly for power and frequency) to average value for assumed length of original signal observation sector:

$$\mathrm{FIF} = \frac{\mathrm{SD}_{\overline{f_{\max}}}}{\overline{f_{\max}}} \tag{4}$$

$$\mathrm{PIF} = \frac{\mathrm{SD}_{\overline{P_{\max\%}}}}{\overline{P_{\max\%}}} \tag{5}$$

The second method of a quantitative spectrogram description consists in the analysis of changes in total PSD of the analysed signal, as a function of time. PSD is being calculated for intervals of an analysing window length, which is being shifted forward by a step equal to 1, Fig. 1b. In each window, total PSD$_T$ has been determined, and next a variability of each total PSD$_T$ as a function of time has been found. PSD$_T$ variability characteristics determined that way are subjected to statistical

analysis, *i.e.* the total PSD maximum value (PSD_{Tmax}), total PSD minimum value (PSD_{Tmin}), the total PSD mean value (PSD_{Tmean}) and total PSD range (PSD_{Trange}) are being determined.

3. Experiment

3.1. Subject

The right eyes of ten subjects were examined in this study. The subjects were in good health, free of any eye pathology. Participants of the experiment agreed to using their study results in the publication.

3.2. Instrumentation

Pupillometric system developed in the Institute of Physics of the Wrocław University of Technology (Poland) was used for recording the dynamics of the SPF signal with 90 Hz frequency. Details of the system structure have been presented in [22, 23].

The system consists of a PC and pupillometer measurement head involving three functional modules: detection, optical and lighting. The measurement head is located inside a black box, assembled at the ophtalmological lamp support. That way of assembling enables us to move the pupillometer head to/from patient's eye, using joystick. CCD camera is used for controlling an eye position against the measurement system. A forehead and chin of a patient are fixed against a head support. The system enables direct recording of the pupillary reaction, which is separately measured for each eye. An eye not being subject to the test is to be covered. A block diagram of the pupillometer is presented in Fig. 2.

An eye being subjected to the test is illuminated with IR radiation, the source of which is a set of 3 diodes arranged in a straight line beneath the tested eye. A pupil view is recorded by the detection system composed of two linear CCD sensors, the one located horizontally and the other at an angle of 90°. The vertical distance between sensors is constant and amounts to $h = 1$ mm. The proposed spatial
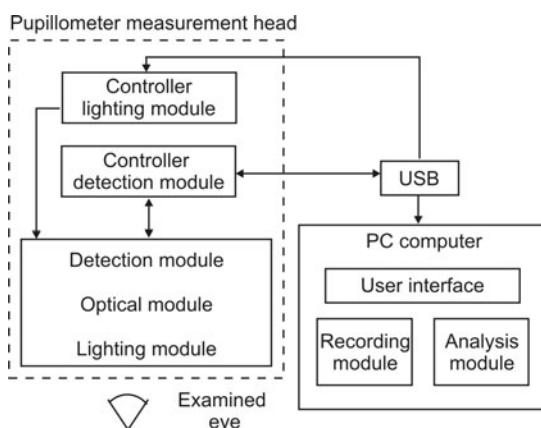

Fig. 2. Block diagram of the pupillometer.

configuration of the CCD sensors allows us to record two, parallel to each other (in distance h), pupillary chords (d_1 and d_2). Using the geometrical sinus theorem and assuming that the measured pupil is circular, the pupil diameter is determined.

A source of fixation is a red LED located at a distance of 30 cm in front of a tested eye.

3.3. Experimental protocol

Before initiating a measurement series, all subjects participated in a training session concerning the pupillometric measuring procedure. Measurements were taken on adapting a patient to darkness (5 min) and calibrating the system to individual characteristics of the subject. A patient was asked to keep his/her eyes open, look at the fixation point, and avoid blinking and head movements during the recording procedure. Patients were also asked to avoid drinking coffee and alcohol for 24 hours before the measuring session. Measuring sessions were conducted between 16:00 and 17:00 hour. Each measurement lasted for 12 seconds, thus the signal length used for the analysis contained 1080 samples.

4. Results

In the article, examples of SPF signals for four selected subjects have been presented (WS – 30 year-old woman; MB – 25 year-old woman; MN – 30 year-old man; JJ – 38 year-old man).

Using the KPSS test, a hypothesis on SPF signal stationarity was studied. In the KPSS test, the following values have been found: 0.320 for WS; 1.374 for MB, 0.547 for MN and 0.252 for JJ. Since the obtained values happened to be greater from the critical value of 0.216, for critical level 0.01, thus the hypothesis on the analyzed signal stationarity has to be rejected.

At a 2-D time-frequency graph for WS (Fig. 3**a**) all subsequent harmonics corresponding to the pulse frequency are clearly seen, but the most important of them are: base component (~1.08 Hz) and harmonics 2nd, 4th, 6th and 8th (~9.7 Hz). At the time-frequency graph it can particularly be observed in the central part of the measuring time interval. In the initial and final parts of the measurement, the proportions between particular harmonics are not that clear, though they are also visible. The spectrum graph, set for up to 20 Hz range (Fig. 3**b**), clearly indicates for the presence of further constituent harmonics. The continuous line represents the spectrum of pupil diameter changes, and the dotted line represents the spectrum of its derivative. Particularly clear and narrow in the frequency range of 10–20 Hz is harmonic 12th (~14 Hz). Figure 3**c** shows that the peak of maximum PSD assumes different values and appears in different frequency ranges. The biggest value has a peak appearing in third time interval for 0.83–1.66 frequency range (~10% PSD value in the whole range). The graph presented in Fig. 3**d** shows that PSD changes occur in the range from 3.61×10^{-3} mm^2/Hz up to 14.08×10^{-3} mm^2/Hz.
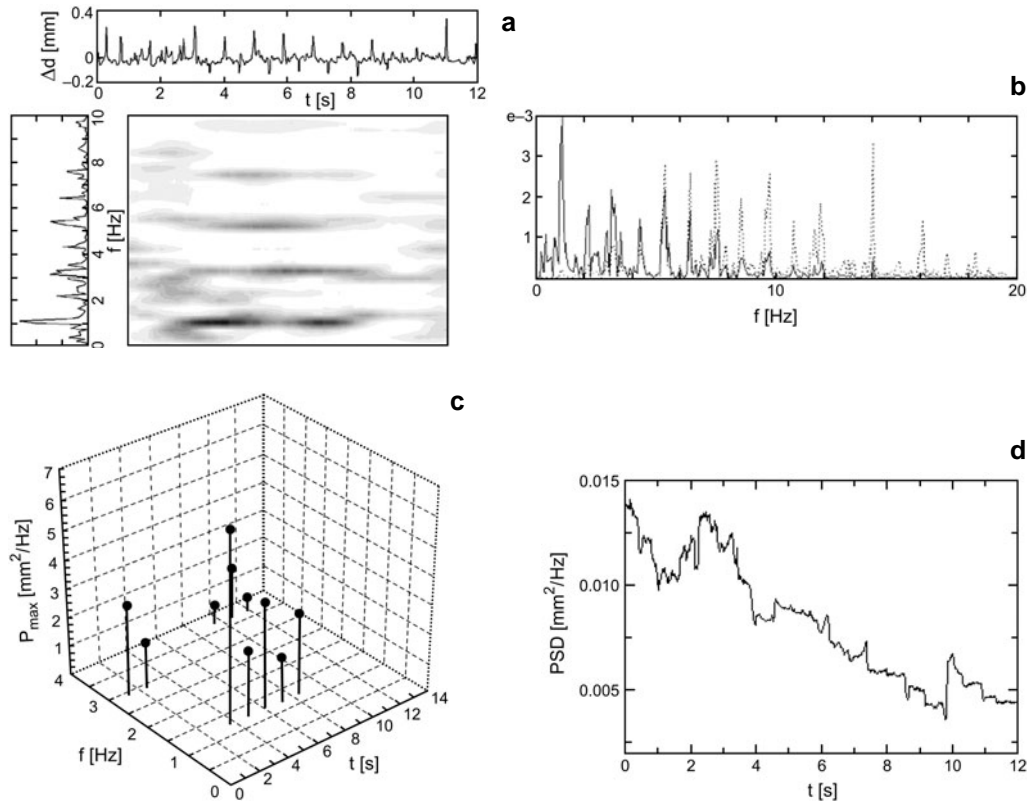
Fig. 3. Results for WS: time-frequency graph of the SPF (**a**), power spectrum SPF and DSPF graph, for up to 20 Hz (**b**), 3D visualization of $P_{i\max}$ changes (**c**) and time graph for PSD function (**d**).

The time-frequency graph for MB pupil diameter changes (Fig. 4**a**) shows clearly the pulse of (~1.1 Hz) and its harmonics (except for the 1st one), up to the 8th one (~9.9 Hz). Pulse harmonic with the highest amplitude, appearing in the graph of pupil diameter changes, is the 2nd one (~3.3 Hz). The course of changes in pupil diameter, in that case from 5th second to the end of measurement, shows clear, periodic, short peaks of fast enlarging of eye pupil. The total change in pupil diameter in that case equals to 0.32mm, for the whole measurement interval.

The spectrum of pupil diameter changes and of its derivative within the range of up to 20 Hz (Fig. 4**b**) indicates here, similarly as in the previous case, the existence of narrow and clearly defined harmonics for frequency above 10 Hz. The clearest ones are 10th (~12.1 Hz), 13th and 14th harmonics (~16.5 Hz). Figure 4**c** shows that max PSD peak appears in the 5th time interval, for the frequency range of 0−0.83 Hz (which constitutes for 5.5% of PSD value within the whole range). Simultaneously, it can be observed that greater part of signal energy is situated in the 2nd part of the signal duration. Most of the signal energy is concentrated in the range of 0−0.83 Hz (~6%),
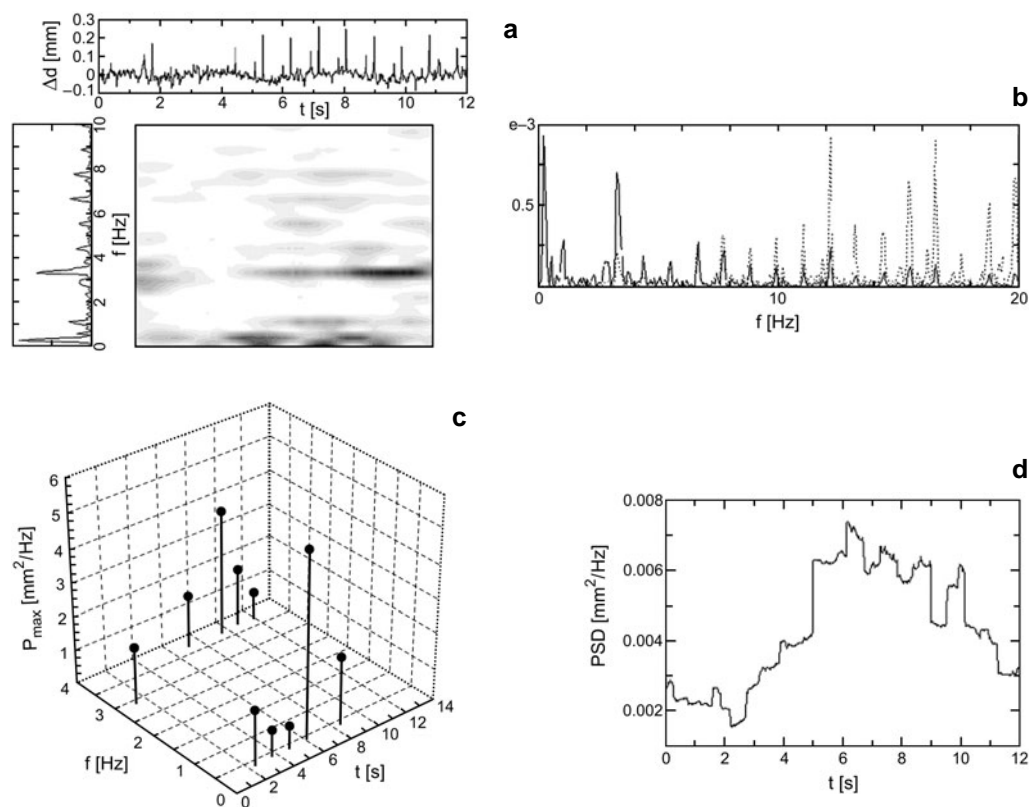
Fig. 4. Results for MB: time-frequency graph of the SPF (**a**), power spectrum SPF and DSPF graph, in the range of up to 20 Hz (**b**), 3D visualization of $P_{i\max}$ changes (**c**), and time graph for PSD function (**d**).

and in the range of 3.32–4.15 Hz (~5%). The graph presented in Fig. 4**d** shows that PSD changes appear in the range from 1.54×10^{-3} mm²/Hz up to 7.39×10^{-3} mm²/Hz.

Figures 5**a** and 6**a** present the graphs of pupil diameter changes for MN and JJ, respectively. The graphs are clearly „more smoothly" in character and do not show fast, shortly lasting changes in pupil diameter. In that case, the spectrum decays fast and higher harmonics do not appear there. That is why the decision was taken to perform the analysis of not the spectrum itself, but of its derivative.

As already mentioned, the spectrum of pupil diameter change speed contains the same frequencies as that of pupil diameter change, but higher frequencies are clearer here, because the spectrum of pupil diameter changes is multiplied in that case by linearly increasing argument (the theorem on Fourier transform and function derivative).

The graph for MN (Fig. 5**b**) does not show clearly the blood pulsing frequency, but the clearest is the 1st harmonic of blood pulse (~2.7 Hz) and the 5th one (~8.2 Hz). For the frequency of about 5 Hz the spectrum fades and there are no frequencies present in that signal. At the graph for JJ (Fig. 6**b**), the frequencies corresponding to blood

pulse are clearly visible (~1.07 Hz), as well as to the 1st, 2nd, 5th and 6th pulse harmonics (~7.5 Hz). Similarly as in the previous case, there are no oscillations for about 5 Hz frequency.

Longitudinal eye movement studies [19] for several patients have shown that in the longitudinal eye oscillation graph, for some subjects, there are no oscillations of around 5 Hz frequency range. It seems that in some way this is a mechanical frequency band prohibited for some patient eye.

While analysing the graph presented in Fig. 5**c** it can be stated that max PSD peak occurs in 1st time interval for 2.49–3.32 frequency range (~6%). Furthermore, in this range most of signal energy is concentrated (total ~22%). The PSD time changes, according to the graph presented in Fig. 5**d**, appear in the range from 0.05×10^{-3} mm^2/s^2/Hz up to 0.13×10^{-3} mm^2/s^2/Hz. Figure 6**c** shows that max PSD peak appears in the 5th time interval, for the frequency range of 3.32–4.15 Hz (~3%). Most of the signal energy is concentrated in the range of 2.49–3.32 Hz and 3.32–4.15 Hz (total ~11%). The graph presented in Fig. 6**d** shows that PSD changes appear in the range from 0.68×10^{-3} mm^2/s^2/Hz up to 4.60×10^{-3} mm^2/s^2/Hz. In DSPF signal spectrum for subjects WS and MB higher pulse harmonics appear (12th – ~14 Hz for WS and 10th – ~12Hz, 13th, 14th – ~16.5 Hz for MB). In DSPF spectrum for MN and JJ, harmonics in the range above 10 Hz have not been observed. Moreover, analysing

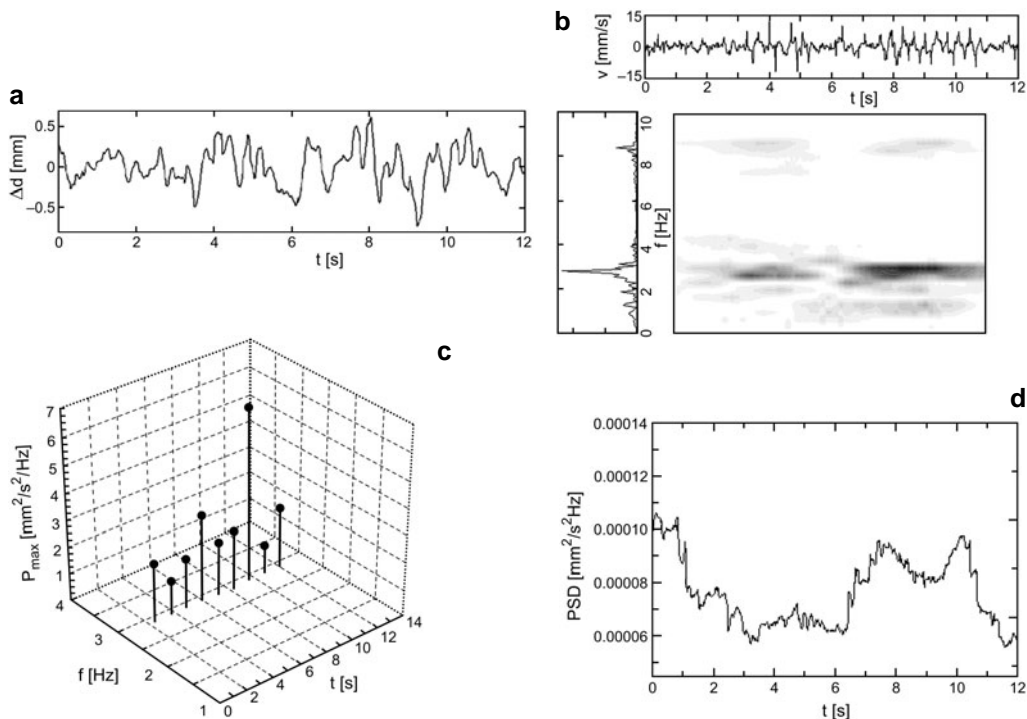Fig. 5. Results for MN: SPF graph (**a**), time-frequency graph of the SPF derivative (**b**), 3D visualization of $P_{i\max}$ changes (**c**) and time graph for PSD function (**d**).

Fig. 6. Results for JJ: SPF graph (**a**), time-frequency graph of the SPF derivative (**b**), 3D visualization of $P_{i\max}$ changes (**c**) and time graph for PSD function (**d**).
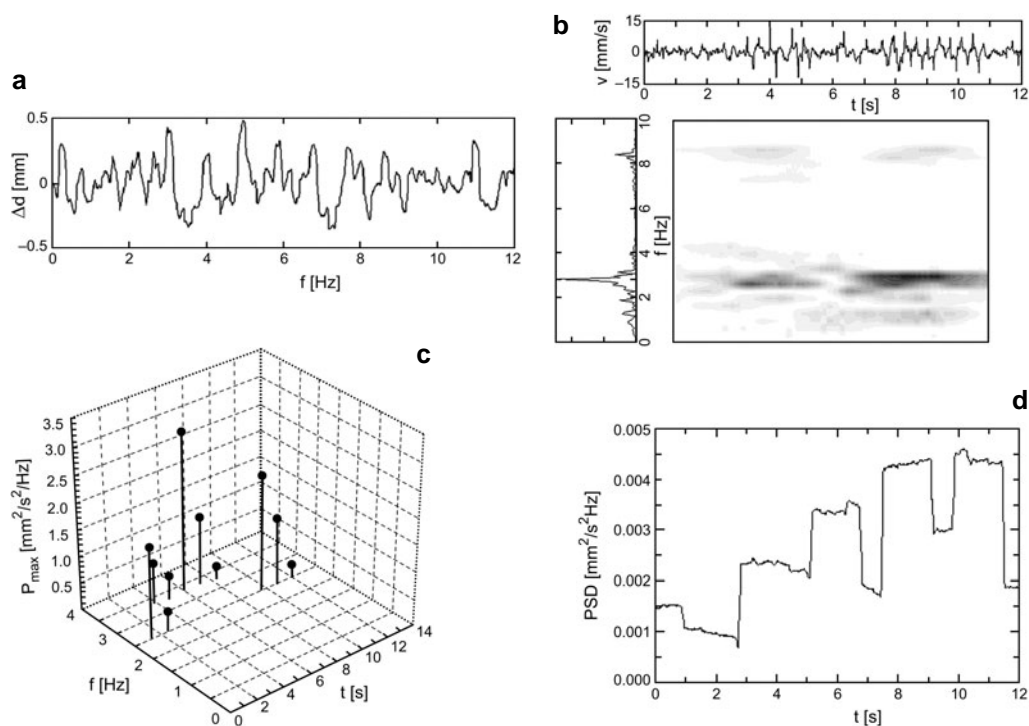
the spectrogram, one can observe that individual harmonics appear irregularly in different time moments, and their time duration is also varying. For example, the base component for JJ lasts from 2nd sec to 8th sec, the 1st harmonic from 1st sec to 4th sec, and the 2nd harmonic from 2nd sec to 9th sec while 6th harmonic from 2nd sec to 8th sec. The Table presents a set of values for the proposed quantitative parameters which describe the obtained spectral characteristics.

5. Discussion and conclusions

The application of fast pupillometry for recording and extended spectral analysis in examining of the SPF signal enables the detection of interesting frequency components in some subjects in the spectrum in the range above 1 Hz. In some cases the harmonics appear even for up to 20 Hz. Moreover, the analysis of the obtained spectrograms shows that the distribution of the PSD amplitude peaks is different for different frequencies. The detection of those irregularities with the use of the classical FT analysis is not possible. The proposed numerical parameters can be used as quantitative measures of the short-lasting time-frequency and time-amplitude variations of the analysed signals. FIF and PIF can be treated as global parameters and their values characterize the fluctuation of amplitude and frequency of the SPF signal spectrum.

T a b l e. Quantitative parameter values for SPF and DSPF signals spectral analysis.

	Parameters	WS	MB	MN	JJ
SPF	PSD_1 [mm^2/Hz]	6.7×10^{-3}	2.9×10^{-3}	14.1×10^{-3}	8.5×10^{-3}
	PSD_2 [mm^2/Hz]	4.4×10^{-3}	0.9×10^{-3}	3.0×10^{-3}	5.4×10^{-3}
	PSD_3 [mm^2/Hz]	16.5×10^{-3}	5.6×10^{-3}	2.4×10^{-3}	18.0×10^{-3}
	PSD_4 [mm^2/Hz]	31.5×10^{-3}	15.7×10^{-3}	19.6×10^{-3}	38.6×10^{-3}
DSPF	PSD_1 [mm^2/s^2/Hz]	0.006×10^{-3}	0.002×10^{-3}	0.010×10^{-3}	0.008×10^{-3}
	PSD_2 [mm^2/s^2/Hz]	0.038×10^{-3}	0.009×10^{-3}	0.032×10^{-3}	0.083×10^{-3}
	PSD_3 [mm^2/s^2/Hz]	2.567×10^{-3}	0.880×10^{-3}	0.164×10^{-3}	3.083×10^{-3}
	PSD_4 [mm^2/s^2/Hz]	6.710×10^{-3}	13.205×10^{-3}	0.301×10^{-3}	9.812×10^{-3}
SPF	FIF/PIF	0.50/0.72	0.84/0.75	0.48/0.68	0.93/0.53
DSPF	FIF/PIF	0.28/0.47	0.34/0.77	0.19/0.69	0.15/0.81
SPF	PSD_{Tmax}[mm^2/Hz]	14.08×10^{-3}	7.39×10^{-3}	6.96×10^{-3}	17.73×10^{-3}
	PSD_{Tmin} [mm^2/Hz]	3.61×10^{-3}	1.54×10^{-3}	2.91×10^{-3}	5.68×10^{-3}
	PSD_{Tmean} [mm^2/Hz]	8.09×10^{-3}	4.33×10^{-3}	4.58×10^{-3}	10.72×10^{-3}
	PSD_{Trange} [mm^2/Hz]	10.47×10^{-3}	5.85×10^{-3}	4.05×10^{-3}	12.04×10^{-3}
DSPF	PSD_{Tmax}[mm^2/Hz]	2.74×10^{-3}	8.12×10^{-3}	0.13×10^{-3}	4.60×10^{-3}
	PSD_{Tmin} [mm^2/Hz]	0.76×10^{-3}	1.07×10^{-3}	0.05×10^{-3}	0.68×10^{-3}
	PSD_{Tmean} [mm^2/Hz]	1.65×10^{-3}	3.93×10^{-3}	0.07×10^{-3}	2.73×10^{-3}
	PSD_{Trange} [mm^2/Hz]	0.008×10^{-3}	7.05×10^{-3}	0.07×10^{-3}	3.92×10^{-3}

Statistical parameters for the PSD time graph can be defined as a measure indicating the PSD variability range. The proposed parameters can be used as a measure of irregularities in the control mechanism responsible for SPF phenomenon.

We are not aware of any work in which the relations were studied. The observed phenomenon may become an inspiration for further, more detailed studies, with the aim of recognising the nature of that phenomenon and finding to what degree it results from an eye structure as a mechanical-optical system, and to what degree it is an effect of nervous control.

References

[1] LOWENSTEIN O., FEINBERG R., LOEWENFELD I.E., *Pupillary movements during acute and chronic fatigue: A new test for the objective evaluation of tiredness*, Investigative Ophthalmology and Visual Science **2**(2), 1963, pp. 138–57.

[2] O'NEILL W.D., OROUJEH A.M., KEEGAN A.P., MERRITT S.L., *Neurological pupillary noise in narcolepsy*, Journal of Sleep Research **5**(4), 1996, pp. 265–71.

[3] MORAD Y., LEMBERG H., YOFE N., DAGAN Y., *Pupillography as an objective indicator of fatigue*, Current Eye Research **21**(1), 2000, pp. 535–42.

[4] PARTALA T., SURAKKA V., *Pupil size variation as an indication of affective processing*, International Journal of Human-Computer Studies **59**(1–2), 2003, pp. 185–98.

[5] Yoss R.E., Moyer N.J., Hollenhorst R.W., *Pupil size and spontaneous pupillary waves associated with alertness, drowsiness and sleep*, Neurology **20**(6), 1970, pp. 545–54.

[6] O'Neill W.D., Oroujeh A.M., Merritt S.L., *Pupil noise is a discriminator between narcoleptics and controls*, IEEE Transactions on Biomedical Engineering **45**(3), 1998, pp. 314–22.

[7] Wilhelm B., Wilhelm H., Lüdtke H., Streicher P., Adler M., *Pupillographic assessment of sleepiness in sleep-deprived healthy subjects*, Sleep **21**(3), 1998, pp. 258–68.

[8] Wilhelm H., Lüdtke H., Wilhelm B., *Pupillographic sleepiness test applied in hypersomniacs and normals*, Graefes Archive for Clinical and Experimental Ophthalmology **236**(10), 1998, pp. 725–9.

[9] Danker-Hopfe H., Kraemer S., Dorn H., Schmidt A., Ehlert I., Herrmann W.M., *Time-of-day variations in different measures of sleepiness-MSLT (pupillography and SSS) and their interrelations*, Psychophysiology **38**(5), 2001, pp. 828–35.

[10] McLaren J.W., Haurib P.J., Siong-Chi Lin, Harris C.D., *Pupillometry in clinically sleepy patients*, Sleep Medicine **3**(4), 2002, pp. 347–52.

[11] Cluydts R., De Valck E., Verstraeten E., Theys P., *Daytime sleepiness and its evaluation*, Sleep Medicine Reviews **6**(2), 2002, pp. 83–96.

[12] Lüdtke H., Wilhelm B., Adler M., Schaeffel F., Wilhelm H., *Mathematical procedures in data recordings and processing of pupillary fatigue waves*, Vision Research **38**(19), 1998, pp. 2889–96.

[13] Wilhelm B., Giedke H., Lüdtke H., Bittner E., Hofmann A., Wilhelm H., *Daytime variations in central nervous system activation measured by a pupillographic sleepiness test*, Journal of Sleep Research **10**(1), 2001, pp. 1–7.

[14] Ohtsuka K., Asakura K., Kawasaki H., Sawa M., *Respiratory fluctuations of the human pupil*, Experimental Brain Research **71**(1), 1988, pp. 215–7.

[15] Yoshida H., Yana K., Okuyama F., Tokoro T., *Time-varying properties of respiratory fluctuations in pupil diameter of human eyes*, Methods of Information in Medicine **33**(1), 1994, pp. 46–8.

[16] Calcagnini G., Lino S., Censi G., Cerutti S., *Cardiovascular autonomic rhythms in spontaneous pupil fluctuations*, Computers in Cardiology **24**, 1997, pp. 133–6.

[17] Censi F., Calcagnini G., De Pasquale F., Lino S., Cerutti S., *Baroceptor-sensitive fluctuations of human pupil diameter*, Computers in Cardiology **26**, 1999, pp. 233–6.

[18] Elsenbruch S., Wang Z., Orr W.C., Chen J.D.Z., *Time-frequency analysis of heart rate variability using short-time Fourier analysis*, Physiological Measurement **21**(2), 2000, pp. 229–40.

[19] Kasprzak H.T., Iskander D.R., *Spectral characteristics of longitudinal corneal apex velocities and their relation to the cardiopulmonary system*, Eye **21**, 2007, pp. 1212–9.

[20] Lin Z., Chen J.D.Z., *Advances in time-frequency analysis of biomedical signals*, Critical Reviews in Biomedical Engineering **24**(1), 1996, pp. 1–72.

[21] Kwiatkowski D., Phillips P.C.B., Schmidt P., Shin Y., *Testing the null hypothesis of stationarity against the alternative of a unit root: How sure are we that economic time series have a unit root?*, Journal of Econometrics **54**(1–3), 1992, pp. 159–78.

[22] Szczepanowska-Nowak W., Hachoł A., Kasprzak H., *System for measurement of the consensual pupil light reflex*, Optica Applicata **34**(4), 2004, pp. 619–34.

[23] Hachol A., Szczepanowska-Nowak W., Kasprzak H., Zawojska I., Dudzinski A., Kinasz R., Wygledowska-Promienska D., *Measurement of pupil reactivity using fast pupillometry*, Physiological Measurement **28**(1), 2007, pp. 61–72.